Chapter 1

The Effect of Split Injection on the Combustion and Emissions in DI and IDI Diesel Engines

S. Jafarmadar

Additional information is available at the end of the chapter

http://dx.doi.org/10.5772/55232

1. Introduction

The major pollutants from diesel engines are NOx and soot. NOx and soot emissions are of concerns to the international community. They have been judged to pose a lung cancer hazard for humans as well as elevating the risk of non-cancer respiratory ailments. These emissions react in the atmosphere in the presence of sunlight to form ground-level ozone. Ground-level ozone is a major component of smog in our cities and in many rural areas as well. In addition, NOx reacts with water, oxygen and oxidants in the atmosphere to form acid rain. Furthermore, the indirect effect of NOx emission to global warming should be noted. It is possible that NOx emission causes an increase secondary emission formation and global warming.

Stringent exhaust emission standards require the simultaneous reduction of soot and NOx for diesel engines, however it seems to be very difficult to reduce NOx emission without increasing soot emission by injection timing. The reason is that there always is a contradiction between NOx and soot emissions when the injection timing is retarded or advanced.

Split injection has been shown to be a powerful tool to simultaneously reduce soot and NOx emissions for DI and IDI diesel engines when the injection timing is optimized. It is defined as splitting the main single injection profile in two or more injection pulses with definite delay dwell between the injections. However, an optimum injection scheme of split injection for DI and IDI diesel engines has been always under investigation.

Generally, the exhaust of IDI diesel engines because of high turbulence intensity is less smoky when compared to DI diesel engines [1]. Hence, investigation the effect of split injection on combustion process and pollution reduction of IDI diesel engines can be quite valuable.

In an IDI diesel engine, the combustion chamber is divided into the pre-chamber and the main chamber, which are linked by a throat. The pre-chamber approximately contains 50% of the combustion volume when the piston is at TDC. This geometrical represents an additional difficulty to those deals with in the DI combustion chambers. Fuel injects into the pre-combustion chamber and air is pushed through the narrow passage during the compression stroke and becomes turbulent within the pre-chamber. This narrow passage speeds up the expanding gases more.

In the recent years, the main studies about the effect of the split injection on the combustion process and pollution of DI and IDI diesel engines are as follows.

Bianchi et al [2] investigated the capability of split injection in reducing NOx and soot emissions of HSDI Diesel engines by CFD code KIVA-III. Computational results indicate that split injection is very effective in reducing NOx, while soot reduction is related to a better use of the oxygen available in the combustion chamber.

Seshasai Srinivasan et al [3] studied the impact of combustion variations such as EGR (exhaust gas recirculation) and split injection in a turbo-charged DI diesel engine by an Adaptive Gradient-Based Algorithm. The predicted values by the modeling, showed a good agreement with the experimental data. The best case showed that the nitric oxide and the particulates could be reduced by over 83% and almost 24%, respectively while maintaining a reasonable value of specfic fuel consumption.

Shayler and Ng [4] used the KIVA-III to investigate the influence of mass ratio of two plus injections and delay dwell on NOx and soot emissions. Numerical conclusions showed that when delay dwell is small, soot is lowered but NOx is increased. In addition, when delay dwell is large, the second injection has very little influence on soot production and oxidation associated with the first injection.

Chryssakis et al [5] studied the effect of multiple injections on combustion process and emissions of a DI diesel engine by using the multidimensional code KIVAIII. The results indicated that employing a post-injection combined with a pilot injection results in reduced soot formation; while the NOx concentration is maintained at low levels.

Lechner et al [6] analyzed the effect of spray cone angle and advanced injection-timing strategy to achieve partially premixed compression ignition (PCI) in a DI diesel engine. The authors proved that low flow rate of the fuel; 60-degree spray cone angle injector strategy, optimized EGR and split injection strategy could reduce the engine NOx emission by 82% and particular matter by 39%.

Ehleskog [7] investigated the effect of split injection on the emission formation and engine performance of a heavy-duty DI diesel engine by KIVA-III code. The results revealed that reductions in NOx emissions and brake-specific fuel consumption were achieved for short dwell times whereas they both were increased when the dwell time was prolonged.

Sun and Reitz [8] studied the combustion and emission of a heavy-duty DI diesel engine by multi-dimensional Computational Fluid Dynamics (CFD) code with detailed chemistry, the

KIVA-CHEMKIN. The results showed that the start of late injection timing in two-stage combustion in combination with late IVC timing and medium EGR level was able to achieve low engine-out emissions.

Verbiezen et al [9] investigated the effect of injection timing and split injection on NOx concentration in a DI diesel engine experimentally. The results showed that advancing the injection timing causes NOx increase. Also, maximum rate of heat release is significantly reduced by the split injection. Hence, NOx is reduced significantly.

Abdullah et al [10] progressed an experimental research for optimizing the variation of multiple injections on the engine performance and emissions of a DI diesel engine. The results show that, the combination of high pressure multiple injections with cooled EGR produces better overall results than the combination of low injection pressure multiple injections without EGR.

Jafarmadar and Zehni [11] studied the effect of split injection on combustion and pollution of a DI diesel engine by Computational Fluid Dynamics (CFD) code. The results show that 25% of total fuel injected in the second pulse, reduces the total soot and NOx emissions effectively in DI diesel engines. In addition, the optimum delay dwell between the two injection pulses was about 25ºCA.

Showry and Rajo [12] carried out the effect of triple injection on combustion and pollution of a DI diesel engine by FLUENT CFD code and concluded that 10° is an optimum delay between the injection pulses for triple injection strategy. The showed that split injections take care of reducing of PM without increasing of NOx level.

As mentioned, the effect of split injection on combustion and emission of DI Diesel engines has been widely studied up to now. However, for IDI diesel engines, the study of split injection strategy in order to reduce emissions is confined to the research of Iwazaki et al [13] that investigated the effects of early stage injection and two-stage injection on the combustion characteristics of an IDI diesel engine experimentally. The results indicated that NOx and smoke emissions are improved by two-stage injection when the amount of fuel in the first injection was small and the first injection timing was advanced from -80 to -100° TDC.

At the present work, the effect of the split injection on combustion and pollution of DI and IDI diesel engines is studied at full load state by the CFD code FIRE. The target is to obtain the optimum split injection case in which the total exhaust NOx and soot concentrations are more reduced than the other cases. Three different split injection schemes, in which 10, 20 and 25% of total fuel injected in the second pulse, have been considered. The delay dwell between injections is varied from 5°CA to 30°CA with the interval 5°CA.

2. Initial and boundry conditions

Calculations are carried out on the closed system from Intake Valve Closure (IVC) at 165°CA BTDC to Exhaust Valve Open (EVO) at 180°CA ATDC. Fig. 1-a and Fig. 1-b show the numerical grid, which is designed to model the geometry of combustion chamber of IDI

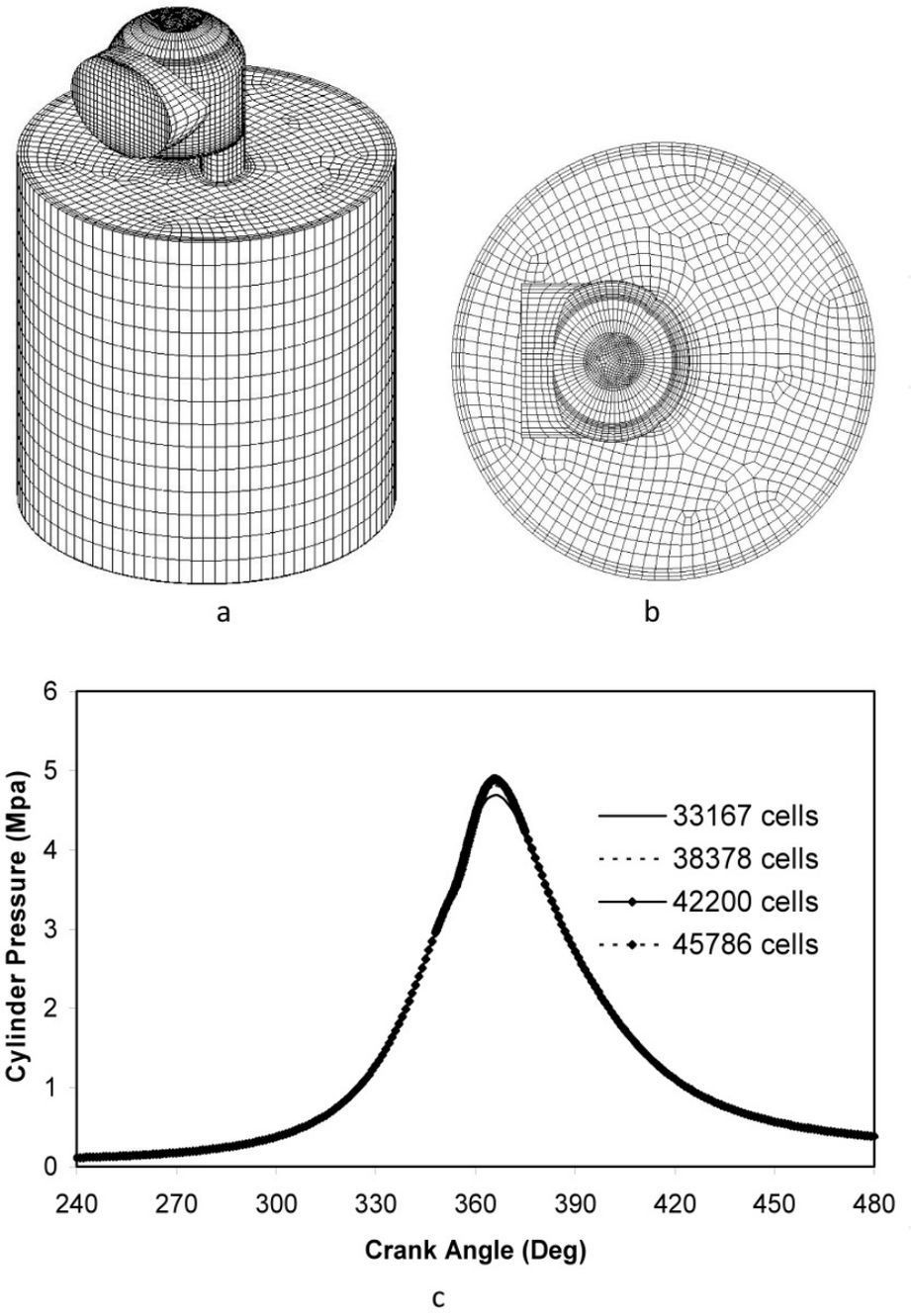

Figure 1. a. Mesh of the Lister 8.1 indirect injection diesel engine; b. Top view of the mesh; c. Grid dependency based on the in-cylinder pressure

engine and contains a maximum of 42200 cells at BTDC. As can be seen from the figure Fig. 1-c, Grid dependency is based on the in-cylinder pressure and present resolution is found to give adequately grid independent results. There is a single hole injector mounted, which is in pre-chamber as shown in fig. 2-a. In addition, details of the computational mesh used in DI are given in Fig. 2-b. The computation used a 90 degree sector mesh (the diesel injector has four Nozzle holes) with 25 nodes in the radial direction, 20 nodes in the azimuthal direction and 5 nodes in the squish region (the region between the top of the piston and the

cylinder head)at top dead center. The ground of the bowl has been meshed with two continuous layers for a proper calculation of the heat transfer through the piston wall. The final mesh consists of a hexahedral dominated mesh. Number of cells in the mesh was about 64,000 and 36,000 at BDC and TDC, respectively. The present resolution is found to give adequately at DI engine. Initial pressure in the combustion chamber is set to 86 kPa and initial temperature is calculated to be 384K, and swirl ratio is assumed to be on quiescent condition. Boundary temperatures for head, piston and cylinder are 550K, 590K and 450K, respectively. Present work is studied at full load mode and the engine speed is 730 rpm. All boundary temperatures were assumed to be constant throughout the simulation, but allowed to vary with the combustion chamber surface regions.

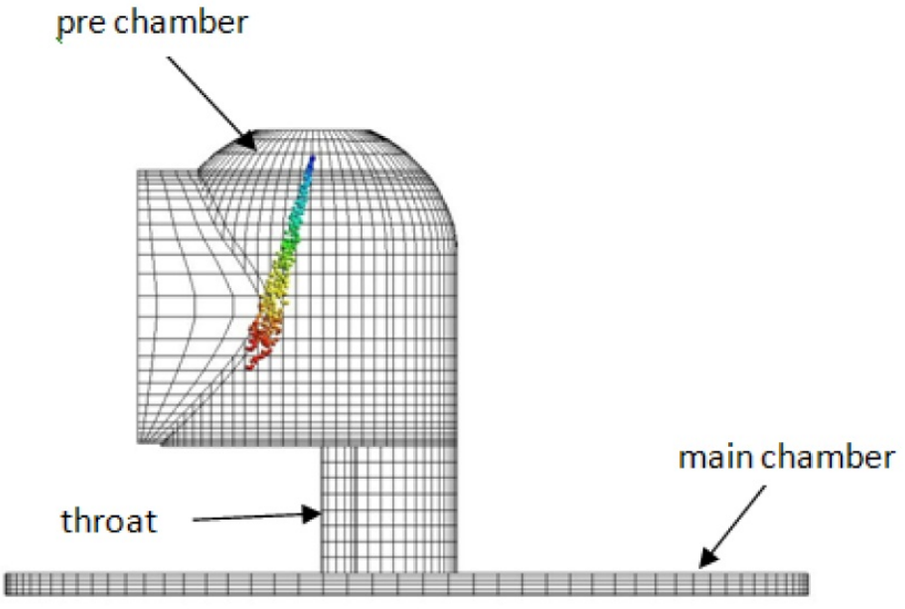

a

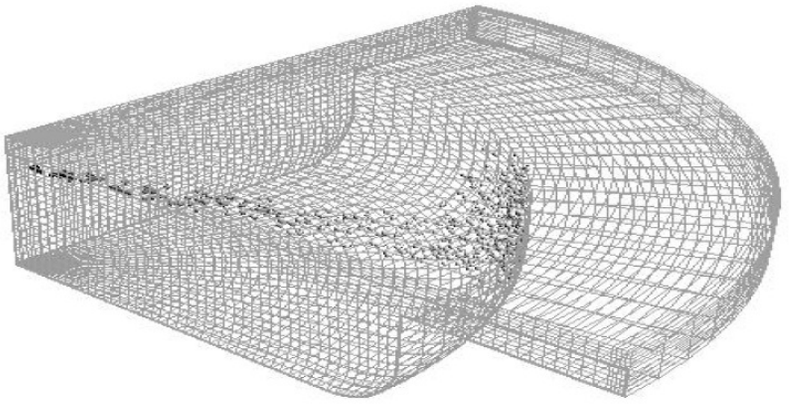

b

Figure 2. a. Spray and injector coordinate at pre-chamber; b Computational mesh with diesel spray drops at 350°CA, single injection case for DI engine.

3. Model formulation

The numerical model is carried out for Lister 8.1 indirect injection diesel engine and OM355 DI engine with the specification given on tables 1 and 2, repectivily. The governing equations for unsteady, compressible, turbulent reacting multi-component gas mixtures flow and thermal fields are solved from IVC to EVO by the commercial AVL-FIRE CFD code [14]. The turbulent flow within the combustion chamber is simulated using the RNG k-ε turbulence model, modified for variable-density engine flows [15].

The standard WAVE model, described in [16], is used for the primary and secondary atomization modeling of the resulting droplets. At this model, the growth of an initial perturbation on a liquid surface is linked to its wavelength and other physical and dynamical parameters of the injected fuel at the flow domain. Drop parcels are injected with characteristic size equal to the Nozzle exit diameter (blob injection).

Cycle Type	Four Stroke
Number of Cylinders	1
Injection Type	IDI
Cylinder Bore	114.1 mm
Stroke	139.7 mm
L/R	4
Displacement Volume	1.43 lit.
Compression Ratio	17.5 : 1
$V_{pre\text{-}chamber}/V_{TDC}$	0.7
Full Load Injected Mass	$6.4336e-5$ kg per Cycle
Power at 850 rpm	5.9 kW
Power at 650 rpm	4.4 kW
Initial Injection Pressure	90 bar
Nozzle Diameter at Hole Center	0.003m
Number of Nuzzle Holes	1
Nozzle Outer diameter	0.0003m
Spray Cone Angle	10°
Valve Timing	IVO= 5° BTDC
	IVC= 15° ABDC
	EVO= 55° BBDC
	EVC= 15° ATDC

Table 1. Specifications of Lister 8.1 IDI diesel engine

The Dukowicz model is applied for treating the heat up and evaporation of the droplets, which is described in [17]. This model assumes a uniform droplet temperature. In addition, the droplet temperature change rate is determined by the heat balance, which states that the heat convection from the gas to the droplet either heats up the droplet or supplies heat for vaporization.

Piston shape	Cylindrical bore
No. of nozzles/injector	4
Nozzle opening pressure	195 (bar)
Cylinders	6, In-line-vertical
Bore * stroke	128 (mm) * 150 (mm)
Max. power	179 (kw) at 2200 (rpm)
Compression ratio	16.1:1
Max. torque	824 N m at 1400 (rpm)
Capacity	11.58 (lit)
IVC	61ºCA after BDC
EVO	60ºCA before BDC
Initial Injection Pressure	250(bar)

Table 2. Engine Specifications of OM-355 Diesel

A Stochastic dispersion model was employed to take the effect of interaction between the particles and the turbulent eddies into account by adding a fluctuating velocity to the mean gas velocity. This model assumes that the fluctuating velocity has a randomly Gaussian distribution [14].

The spray/wall interaction model used in this simulation was based on the spray/wall impingement model [18]. This model assumes that a droplet, which hits the wall was affected by rebound or reflection based on the Weber number.

The Shell auto-ignition model was used for modeling of the auto ignition [19]. In this generic mechanism, six generic species for hydrocarbon fuel, oxidizer, total radical pool, branching agent, intermediate species and products were involved. In addition, the important stages of auto ignition such as initiation, propagation, branching and termination were presented by generalized reactions, described in [14, 19].

The Eddy Break-up model (EBU) based on the turbulent mixing is used for modeling of the combustion in the combustion chamber [14]. This model assumes that in premixed turbulent flames, the reactants (fuel and oxygen) are contained in the same eddies and are separated from eddies containing hot combustion products. The rate of dissipation of these eddies determines the rate of combustion. In other words, chemical reaction occurs fast and the combustion is mixing controlled. NOx formation is modeled by the Zeldovich mechanism and Soot formation is modeled by Kennedy, Hiroyasu and Magnussen mechanism [20].

The injection rate profiles are rectangular type and consists of nineteen injection schemes, i.e. single injection and eighteen split injection cases(as shown in table 4). To simulate the split injection, the original single injection profile is divided into two injection pulses without altering the injection profile and magnitude. Fig. 3 illustrates the schematic scheme of the single and split injection strategy.

For the single injection case, the start of injection is at 348°CA and injection termination is at 387°CA. For all split injection cases, the injection timing of the first injection pulse is fixed at

348°CA. Three different split injection schemes, in which 10-20-25% of total fuel injected in the second pulse, has been considered. The delay dwell between injections is varied from 5°CA to 30°CA with the interval 5°CA.

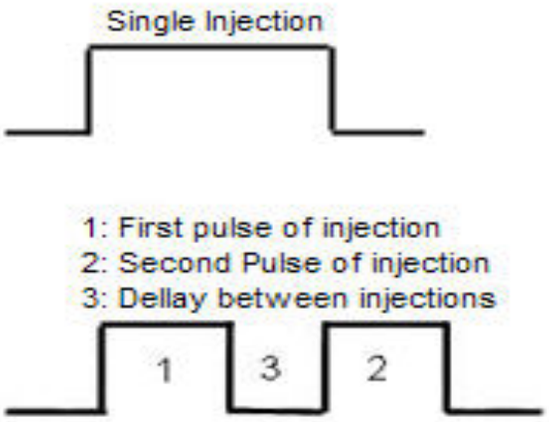

Figure 3. schematic scheme of single and split injection strategy.

4. Performance parameters

Indicated work per cycle is calculated from the cylinder pressure and piston displacement, as follows:

$$W = \int_{\theta_1}^{\theta_2} PdV \tag{1}$$

Where θ1, θ2 are the start and end of the valve-closed period, respectively (i.e. IVC= 15° ABDC and EVO= 55° BBDC). The indicated power per cylinder and indicated mean effective pressure are related to the indicated work per cycle by:

$$P(kW) = \frac{W(N.m)N(rpm)}{60000n} \tag{2}$$

$$IMEP = \frac{W}{V_d} \tag{3}$$

Where n=2 is the number of crank revolutions for each power stroke per cylinder, N is the engine speed in rpm and Vd is volume displacement of piston. The brake specific fuel consumption (BSFC) is defined as:

$$BSFC = \frac{\dot{m}_f}{p_b} \tag{4}$$

In Equation (1), the work is only integrated as part of the compression and expansion strokes; the pumping work has not been taken into account. Therefore, the power and

(ISFC) analyses can only be viewed as being qualitative rather than quantitative in this study.

5. Results and discussion IDI

Fig. 4 and Fig. 5 show the verification of computed and measured [21] mean in-cylinder pressure and heat release rate for the single injection case. They show that both computational and experimental data for cylinder pressure and heat release rate during the compression and expansion strokes are in good agreement.

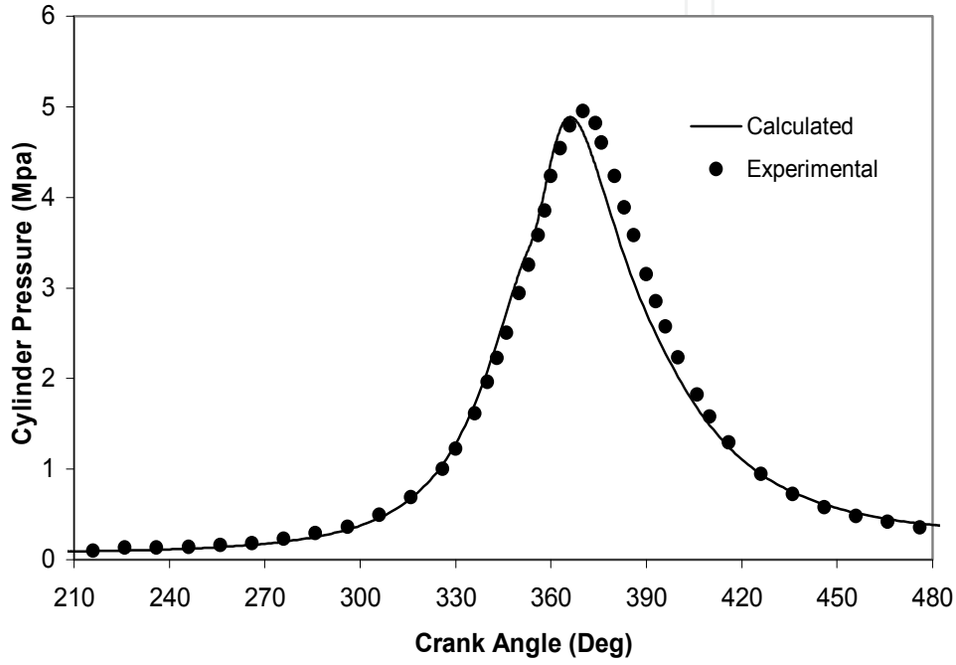

Figure 4. Comparison of calculated and measured [21] in-cylinder pressure, single injection case

The peak of cylinder Pressure is 4.88 Mpa, which occurs at 366°CA (4°CA after TDC). The start of heat release is at 351°CA for computed and measured results; in other words, the ignition delay dwell is 3°CA. It means that the ignition delay is quite close to the chemical ignition delay and that the physical ignition delay is very short, because of the rapid evaporation of the small droplets injected through the small injector gap at the start of injection. The heat release rate, which called "measured", is actually derived from the procured in-cylinder pressure data using a thermodynamic first law analysis as followed:

$$\frac{dq}{d\theta} = \frac{\gamma}{\gamma - 1} p \frac{dV}{d\theta} + \frac{1}{\gamma - 1} V \frac{dp}{d\theta} \tag{5}$$

Where p and V are in-cylinder pressure and volume versus the crank angle θ, and γ=1.33.The main difference of computed and measured HRR is due to applying single zone model to combustion process with assuming γ=1.33 and observed at premixed combustion. The peak of computed HRR is 59J/deg that occurs at 364°CA, compared to the peak of

measured HRR that is 53J/deg at 369°CA. The main validation is based on pressure in cylinder.

As a whole, the premixed combustion occurs with a steep slope and it can be one of the major sources of NOx formation.

Table 3 shows the variation of performance parameters for the single injection case, compared with the experimental data [21]. In contrast with the experimental results, it can be seen that model can predict the performance parameters with good accuracy.

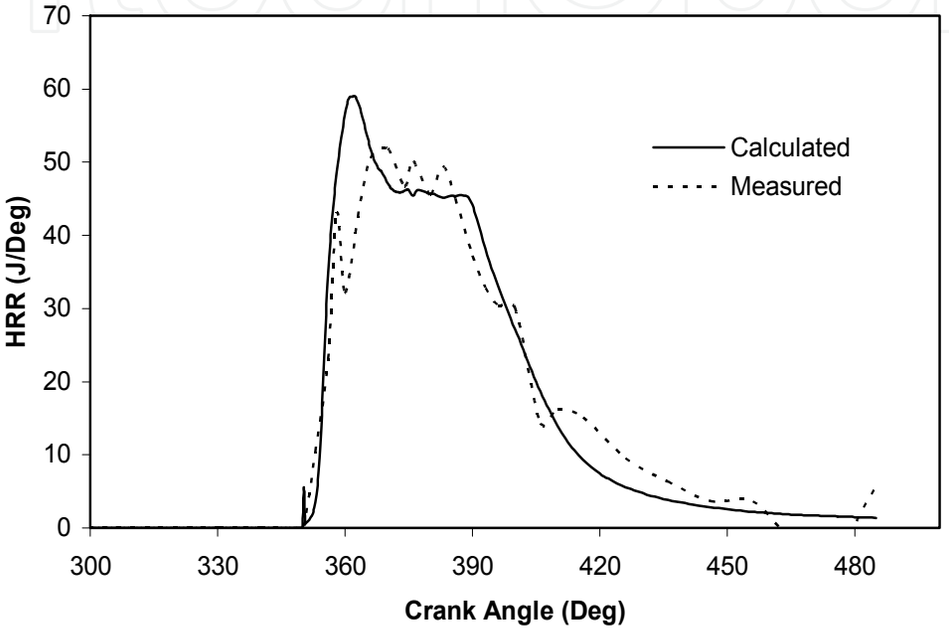

Figure 5. Comparison of calculated and measured [21] heat release rate, single injection case

parameters	Calculated	Experimental
Brake Power [kW]	4.53	4.65
BMEP [Bar]	5.33	5.47
Bsfc [g/kW.h]	310.72	302.7

Table 3. Comparison of calculated and measured [21] performance parameters, single injection case

Fig. 6 indicates that the predicted total in-cylinder NOx emission for the single injection case, agrees well with the engine-out measurements [21]. Heywood [22] explains that the critical time for the formation of oxides of nitrogen in compression ignition engines is between the start of combustion and the occurrence of peak cylinder pressure when the burned gas temperatures are the highest. The trend of calculated NOx formation in the prechamber and main chambers agrees well with the Heywood's explanations. As temperature cools due to volume expansion and mixing of hot gases with cooler burned gas, the equilibrium reactions are quenched in the swirl chamber and main chamber.

As can be seen from the Fig. 7, the predicted total in-cylinder soot emission for the single injection case agrees well with the engine-out measurements [21].

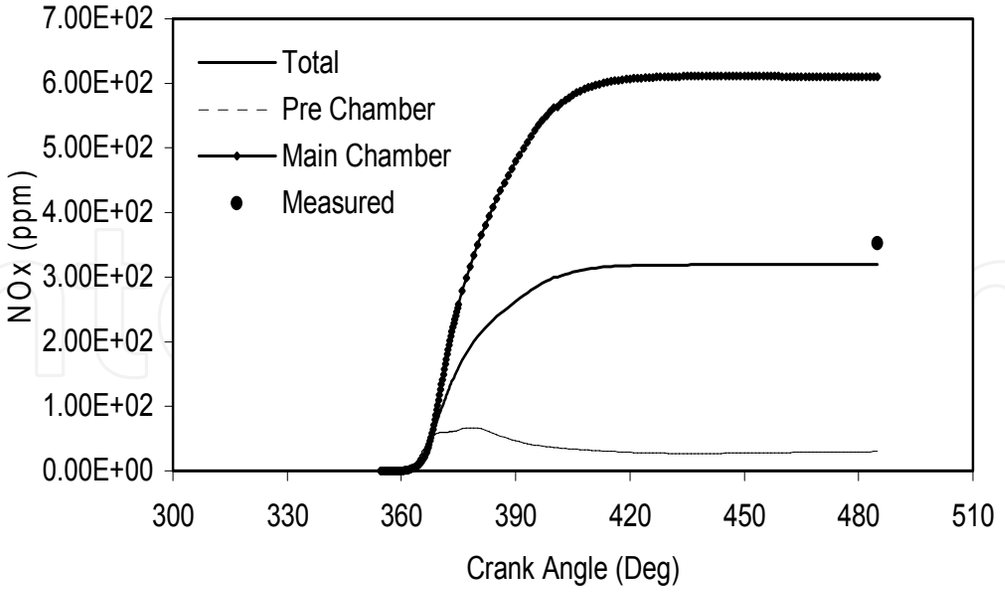

Figure 6. Comparison of calculated and measured [21] NOx emission, single injection case

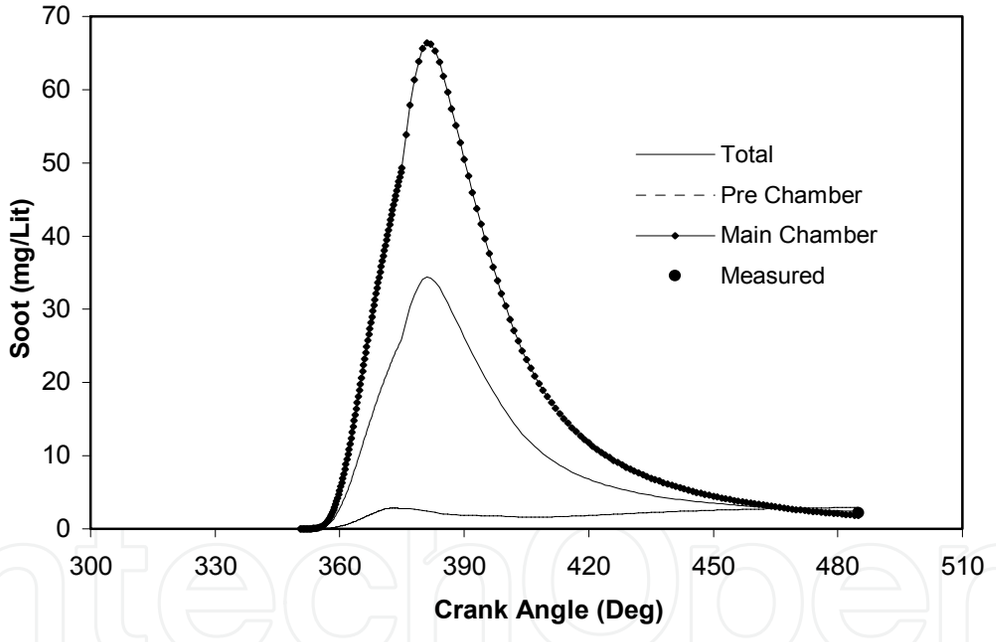

Figure 7. Comparison of calculated and measured [21] Soot emission, single injection case

Table 3 presents the exhaust NOx and soot emissions and performance parameters for the calculated single injection, and split injection cases. As can be seen, the lowest NOx and Soot emissions are related to the 75%-15-25% and 75%-20-25% cases respectively. In order to obtain the final optimum case, i.e. the case that involves the highest average of NOx and Soot reduction, a new dimensionless parameter is defined as:

The more of the total average emission reduction percentage results to the better optimum split injection case. Hence, it is concluded that the 75%-20-25% scheme with the average reduction percentage of 23.28 is the optimum injection case.

In addition, it can be deduced from the table 4 that in general, split injection sacrifices the brake power and Bsfc of the engine. This result is more apparent for the 80%-20% and 75%-25% cases. The reason is that with reduction of the first pulse of injection and increase of delay dwell between injections, premixed combustion as the main source of the power stroke is decreased. Hence, Bsfc is increased as well. As can be seen, the lowest brake power and highest Bsfc are related to the 75%-30-25% case.

Fig. 8 shows the NOx versus Soot emission for the single injection and split injection cases. As can be seen, the 75%-20-25% case is closer to origin, I, e. zero emission. Hence, this confirms that the case of 75%-20-25% is the optimum case.

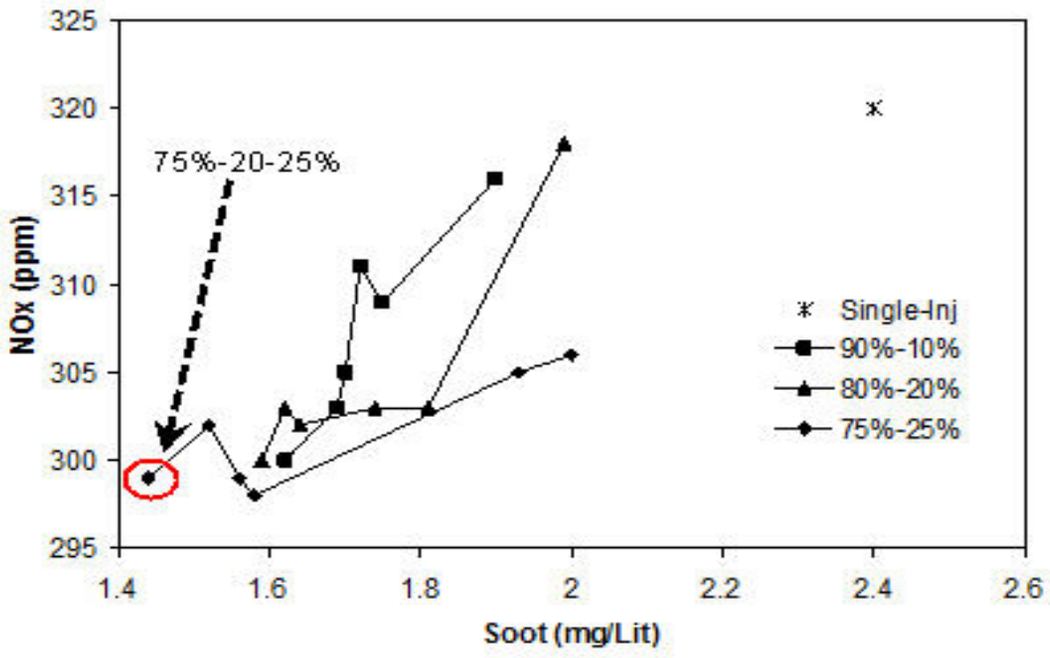

Figure 8. NOx versus soot emission for the single injection and split injection cases

It is of interest to notify that the optimum injection scheme for DI diesel engine at full load state is 75%-25-25% [11]. It means that the first and second injection pulses for the DI and IDI diesel engines are the same. The difference is related to the delay dwell between injections. I.e. the delay dwell for the optimum IDI split injection case is 5°CA lower than that of DI because of high turbulence intensity and fast combustion.

It is noticeable to compare the spray penetration, in-cylinder flow field, combustion and emission characteristics of the single injection and optimum injection cases to obtain valuable results.

The normalized injection profile versus crank angle for the single injection and 75%-20-25% cases is shown in the fig. 9. In this profile, actual injection rate values divided to maximum injection rate and this normalized injection rate profile is used by CFD code.

	NOx (ppm)	Soot (mg/lit)	NOx Reduction (%)	Soot Reduction (%)	Average reduction (%)	Pb (kW)	Bsfc (gr/kw.h)
Single Inj	320	2.4	0	0	0	4.53	310.72
90%-5-10%	316	1.9	1.25	20.83	11.04	4.51	312.1
90%-10-10%	309	1.75	3.43	27.08	15.25	4.4	319.9
90%-15-10%	300	1.62	6.25	32.5	19.37	4.32	325.8
90%-20-10%	311	1.72	2.81	28.33	15.57	4.37	322.1
90%-25-10%	303	1.69	5.31	29.58	17.44	4.33	325.08
90%-30-10%	305	1.7	4.68	29.16	16.92	4.35	323.58
80%-5-20%	318	1.99	0.6	17.08	8.84	4.36	322.84
80%-10-20%	303	1.81	5.31	24.58	14.94	4.31	326.58
80%-15-20%	303	1.74	5.31	27.5	16.4	4.2	335.14
80%-20-20%	302	1.64	5.62	31.66	18.64	4.14	340
80%-25-20%	303	1.62	5.31	32.5	18.9	4.13	340.82
80%-30-20%	300	1.59	6.25	33.75	20	4.12	341.65
75%-5-25%	306	2	4.37	20	12.18	4.29	328.11
75%-10-25%	305	1.93	4.68	19.58	12.13	4.18	336.74
75%-15-25%	**298**	1.58	6.87	34.16	20.51	4.12	341.65
75%-20-25%	299	**1.44**	6.56	40	**23.28**	4.04	348.41
75%-25-25%	302	1.52	5.62	36.66	21.14	4	351.9
75%-30-25%	299	1.56	6.56	35	20.78	3.97	354.55

Table 4. Exhaust emissions and performance parameters for the single injection and split injection cases

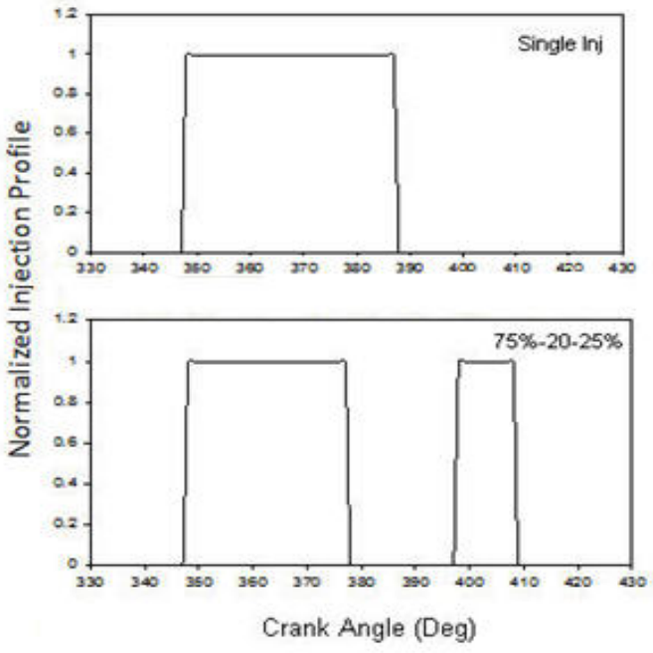

Figure 9. The normalized injection profile versus crank angle for the single injection and 75%-20-25% cases

Fig. 10-a and Fig. 10-b represent respectively front and top views of the evolution of the spray penetration and velocity field at various crank angles in horizontal planes of the pre and main combustion chambers and planes across the connecting throat for the single injection and 75%-20-25% cases. It can be seen that the maximum velocity in throat section are lower at all crank angles because of the large area this section than the other data in the literatures [23]. Generally, for all the cases, the maximum velocity of the flow field is observed at the tip of the spray, swirl chamber throat and some areas of the main chamber that is far from the cylinder wall and cylinder head.

As can be seen, at various crank angles, the main difference of the in-cylinder flow field between the single injection and split injection cases is due to the fuel injection scheme. In other words, the amount of the fuel spray and the crank position in which the spray is injected. The aerodynamic forces decelerate the droplets for the both cases. The drops at the spray tip experience the strongest drag force and are much more decelerated than droplets that follow in their wake.

At 370°CA, air entrainment into the fuel spray can be observed for the both cases. Hence, Droplet velocities are maximal at the spray axis and decrease in the radial direction due to interaction with the entrained gas.

Although the amount of the fuel spray for the single injection case is higher than the 75%-20-25% case at 370°CA, the flow field difference is not observed obviously. The more quantity of the fuel spray for the single injection case causes the maximum velocity of the single injection case to be higher by about 1m/s than the 75%-20-25% case.

At 380°CA, the fuel spray is cut off for the 75%-20-25% case. Since the entrained gas into to the spray region is reduced, the flow moves more freely from the swirl chamber to the main chamber. Hence, as can be seen from the front view, the maximum flow field velocity for the 75%-20-25% case is higher compared to the single injection case.

At 390°CA, from the top view, the distribution of the flow field in the whole of the main chamber is visible. In addition, some local swirls can be seen in the main chamber that are close to the swirl chamber. From the front view, it is observed that the gas coming from the pre-chamber reaches the opposite sides of cylinder wall. This leads to the formation of the two eddies occupying each one-half of the main chamber and staying centered with respect to the two half of the bowl.

The start of the second injection pulse for the 75%-20-25% case is observed At 400°CA. since the swirl intensity in the swirl chamber is reduced at this crank position, the interaction between the flow field and spray is decreased to somehow and flow in the pre-chamber is not strongly influenced by the fuel spray. Hence, the maximum velocity of the flow field for the 75%-20-25% case remains lower compared to the single injection case.

Fig. 11 indicates the history of heat release rate, cylinder pressure, temperature, O2 mass fraction, NOx and soot emissions for the single injection and 75%-20-25% cases.

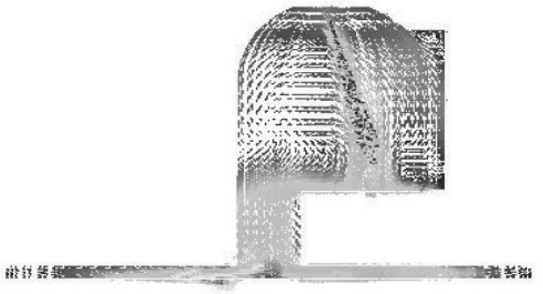

370°CA: Single Inj, V_{max}=56m/s

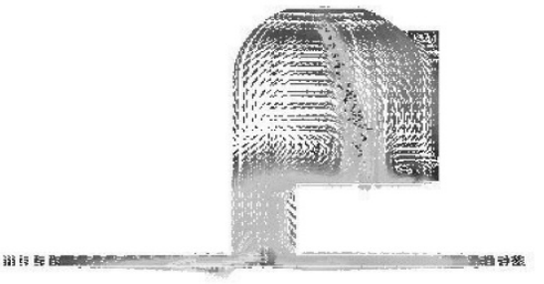

370°CA: 75%-20-25%, V_{max}=55m/s

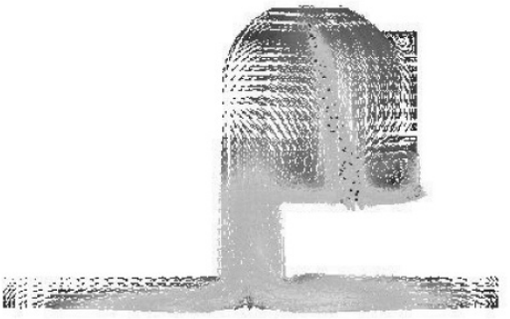

380°CA: Single Inj, V_{max}=41m/s

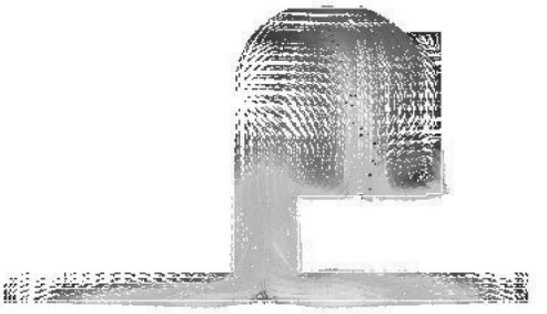

380°CA: 75%-20-25%, V_{max}=42m/s

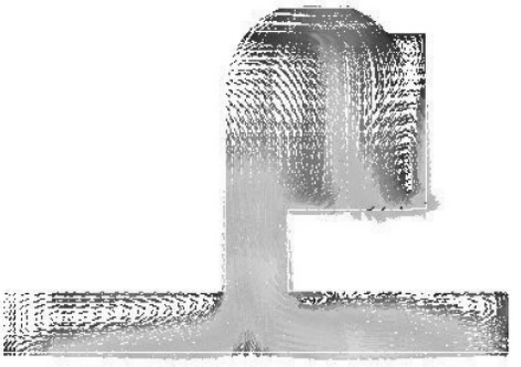

390°CA: Single Inj, V_{max}=40m/s

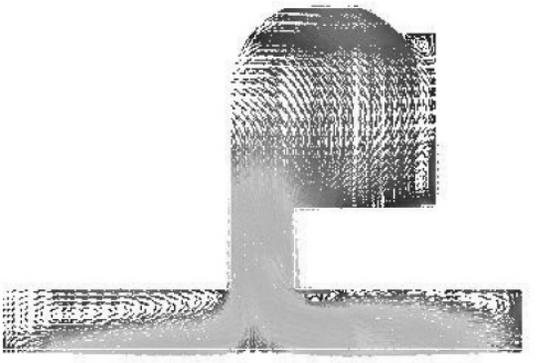

390°CA: 75%-20-25%, V_{max}=36m/s

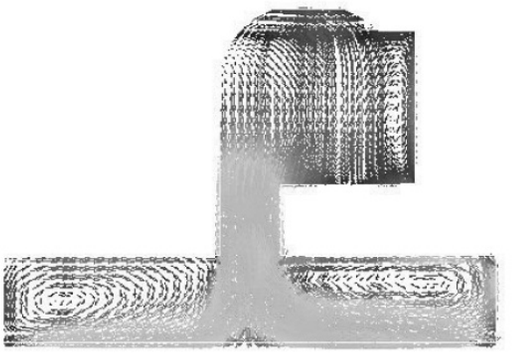

400°CA: Single Inj, V_{max}=35m/s

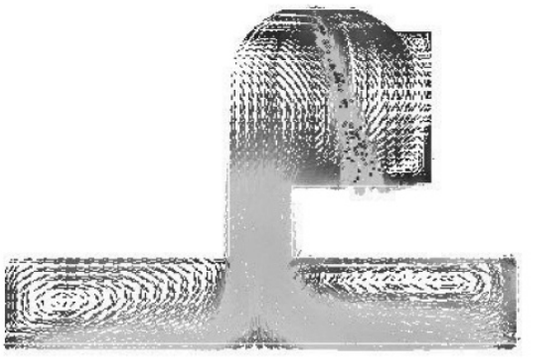

400°CA: 75%-20-25%, V_{max}=30m/s

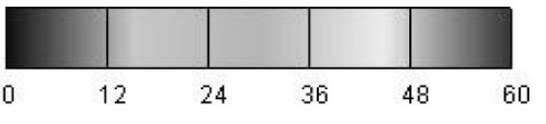

a

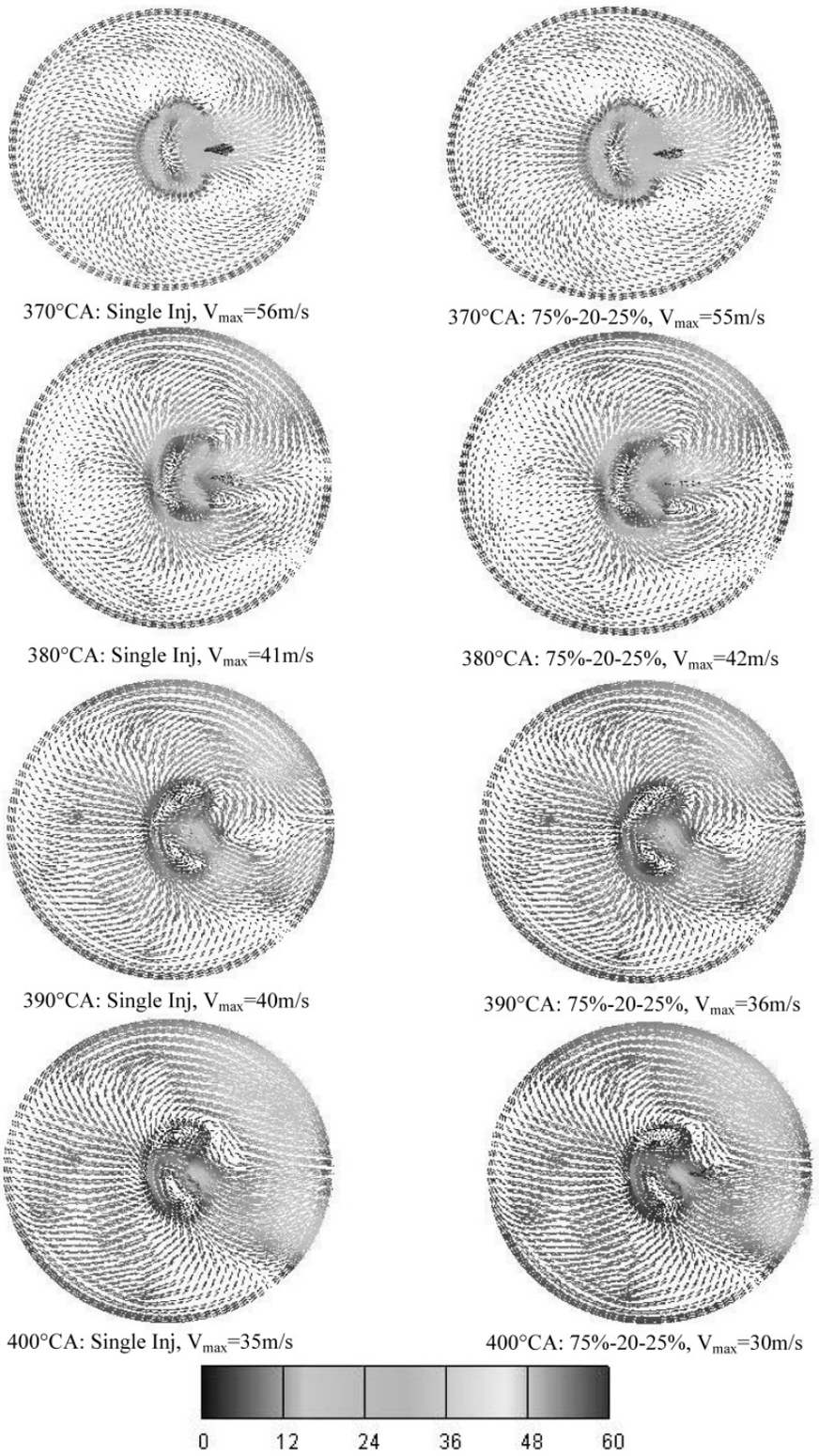

Figure 10. a. Comparison of spray penetration and velocity filed at various crank angles for the single injection and 75%-20-25% cases, front view; b. Comparison of spray penetration and velocity filed at various crank angles for the single injection and 75%-20-25% cases, top view.

Fig. 11-a shows that the amount of heat release rate for the both cases is to somehow equal until 380°CA. It is due to the fact that the first injection pulse for the 75%-20-25% case, lasts to 377°CA. Hence, the premixed combustion for the both cases does not differ visibly. For the 75%-20-25% case, The second peak of heat release rate occurs at 410°CA and indicates that a rapid diffusion burn is realized at the late combustion stage and it affects the in-cylinder pressure, temperature and soot oxidation.

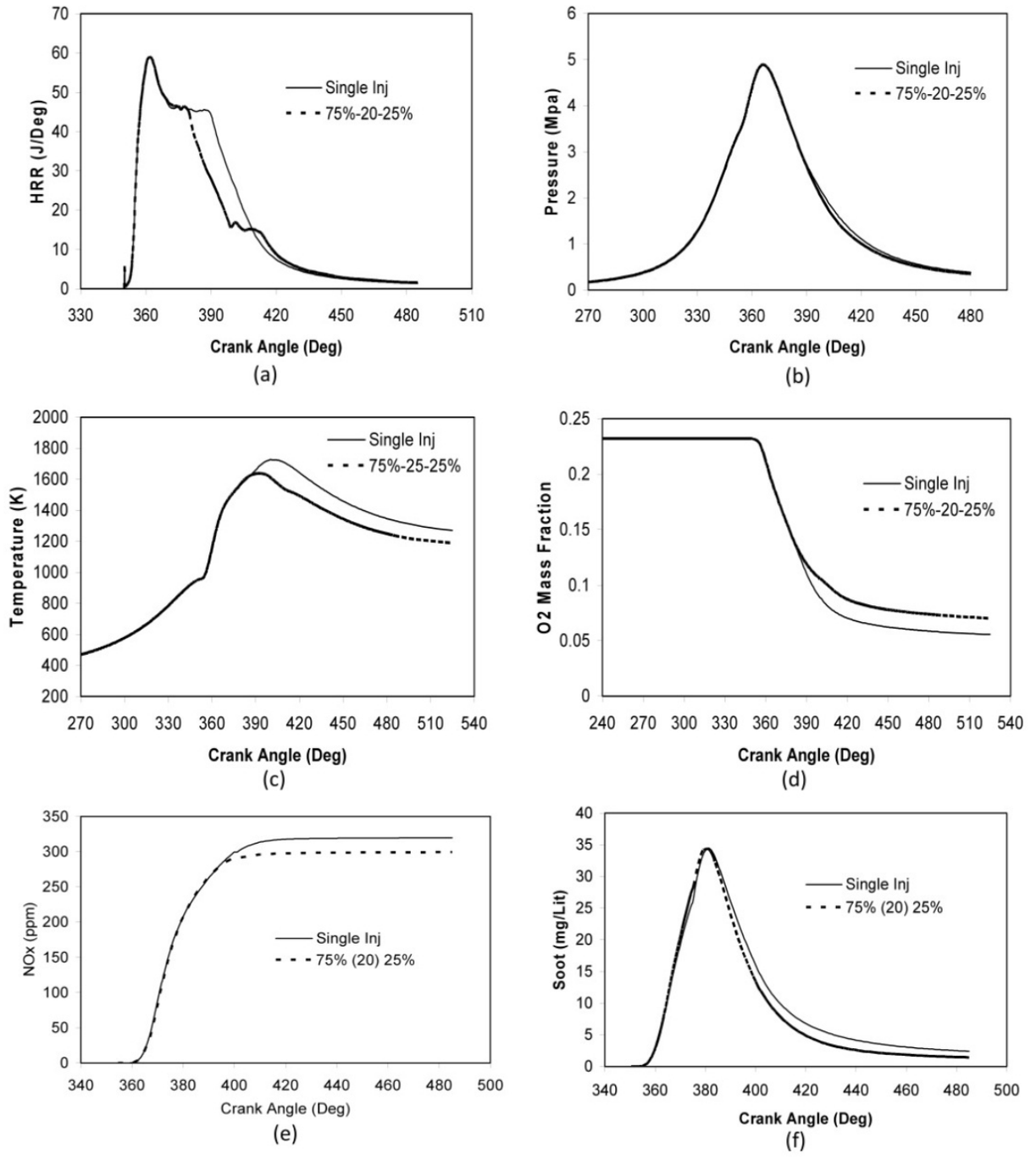

Figure 11. Comparison of HRR, cylinder pressure and temperature, O2 mass fraction, NOx and soot histories for the single injection and 75%-20-25% cases

Fig. 11-b shows that the second injection pulse of the 75%-20-25% does not cause to the second peak of the cylinder pressure. It is because the rate of decrease of cylinder pressure due to the expansion stroke is almost equal to the rate of increase of cylinder pressure due to the diffusion combustion.

Fig. 11-c compares temperature trend for 75%-20-25% and single injection cases. As can be seen, for the 75%-20-25% case, the peak of the temperature advances about 11°CA compared to the peak of the temperature of the single injection case. In addition, the temperature reduction reaches to 90°K.

Fig. 11-d presents the in cylinder O_2 mass fraction. It can be seen that after 385°CA, the O2 concentration for the 75%-20-25% case is higher than that for the single injection case. In other words, oxygen availability of 75%-20-25% case is better.

As Fig. 11-e and Fig. 11-f indicate, the reduction of the peak of the cylinder temperature for the 75%-20-25% case, causes to the lower NOx formation. In addition, soot oxidation for the 75%-20-25% case is higher compared to that for the single injection case. It is because for the 75%-20-25% case, the more availability of oxygen in the expansion stroke compensates the decrease of temperature due to the split injection. Hence, soot oxidation is increased.

Fig. 12-a and Fig. 12-b represent respectively front and top views of the contours of equivalence ratio, temperature, NOx and soot emissions at various crank angles in horizontal planes of the main combustion chamber and planes across the connecting throat for the single injection and 75%-20-25% cases.

At 400°CA, for the both cases, the majority of NOx is located in the two half of the main chamber, whilst soot is concentrated in the swirl chamber, throat section and main chamber. For the both cases, a local soot-NOx trade-off is evident in the swirl chamber, as the NOx and soot formation occur on opposite sides of the high temperature region. Equivalence ratio contour of the 75%-20-25% case confirms that injection termination and resumption, causes leaner combustion zones. Hence, the more reduction of soot for the 75%-20-25% is visible compared to the single injection case.

NOx and soot formation depend strongly on equivalence ratio and temperature. It is of interest to notice that the area which the equivalence ratio is close to 1 and the temperature is higher than 2000 K is the NOx formation area. In addition, the area which the equivalence ratio is higher than 3 and the temperature is approximately between 1600 K and 2000 K is the Soot formation area. The area from 1500 K and equivalence ratio near to 1 is defined as soot oxidation area [24, 25].

At 410°CA, due to the second injection pulse, increase of the equivalence ratio is observed in the swirl chamber of the 75%-20-25% case. Hence, the enhancement of the soot concentration close to the wall spray impingement is observed. For the other areas, soot oxidation for the 75%-20-25% case is higher compared to the single injection case. In addition, NOx reduction tendency is visible in the right side of the main chamber of the 75%-20-25% case compared to the single injection case. It is because more temperature reduction occurs for the 75%-20-

25% case due to the lower premixed combustion. The diffusion combustion of the second injection pulse does not affect NOx formation significantly.

The final form of the distribution of equivalence ratio, temperature, NOx and soot contours can be seen at 420°CA. The reduction of soot and NOx for the 75%-20-25% case is clear compared to the single injection case. This trend is preserved for the both cases until EVO.

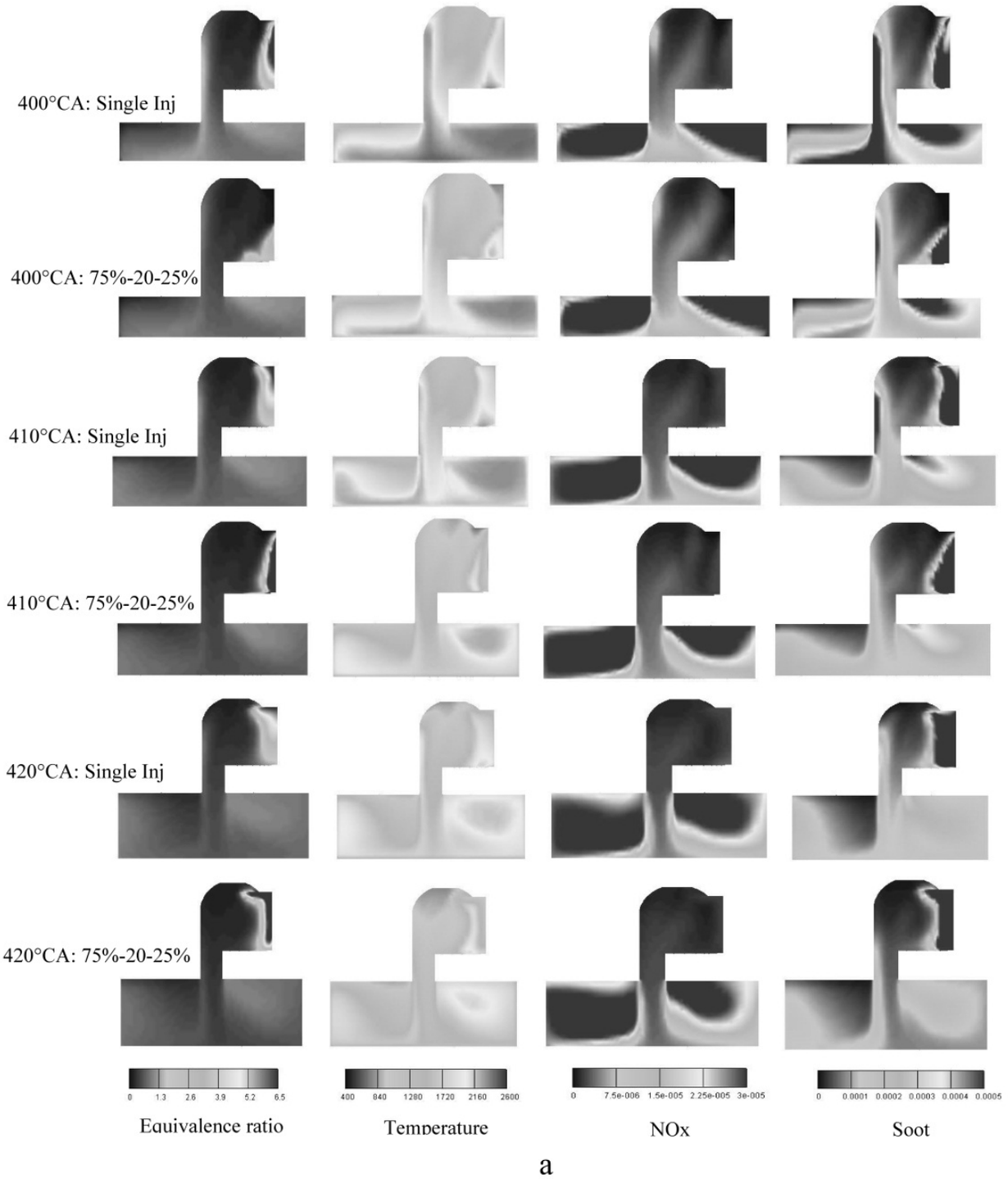

a

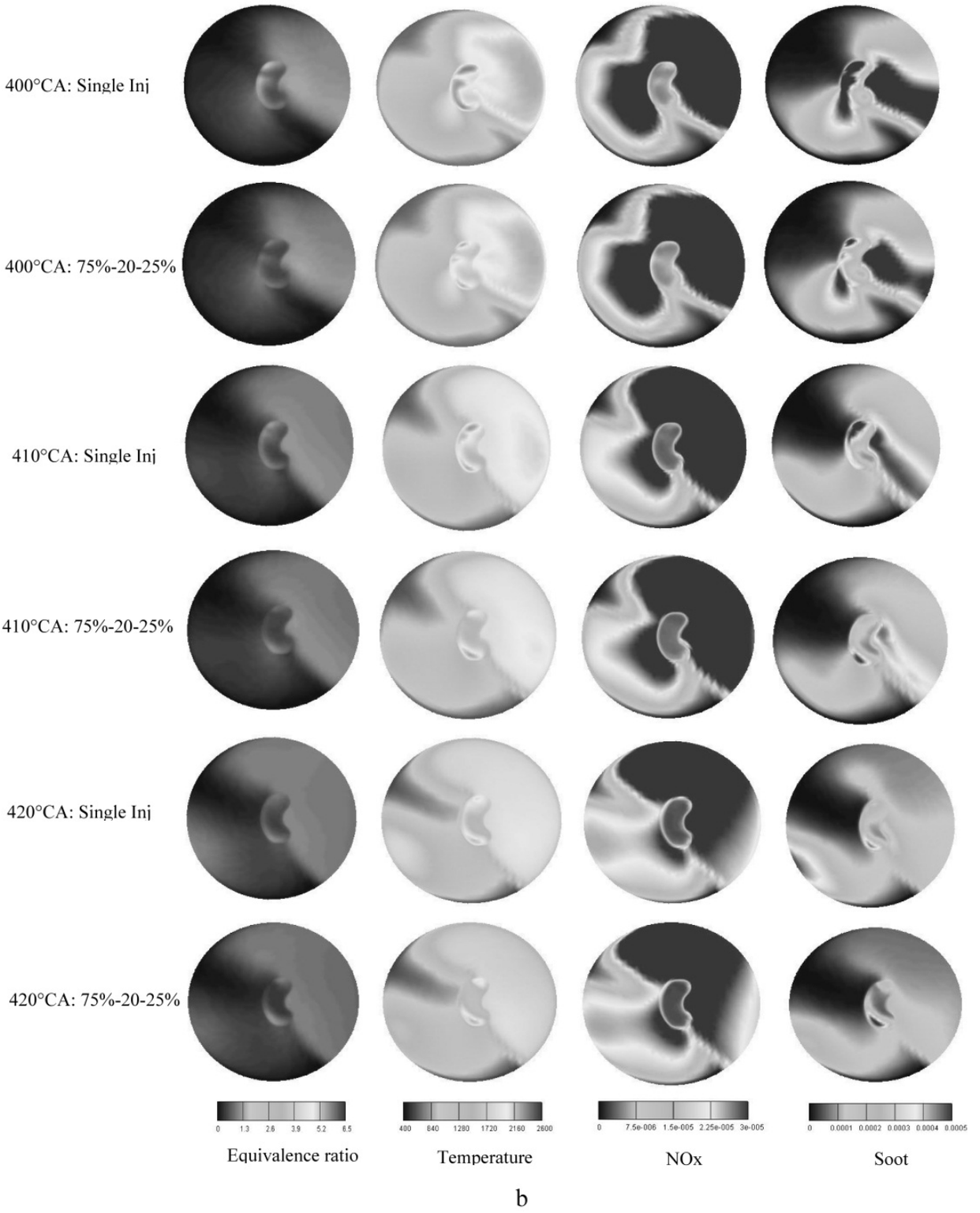

Figure 12. a. Contours of equivalence ratio, temperature, NOx and Soot at different crank angles, front view b. Contours of equivalence ratio, Temperature, NOx and Soot at different crank angles, top view

6. Results and discussion of DI diesel engine

Fig. 13 shows the cylinder pressure and the rate of heat release for the single injection case. As can be seen from HRR curve, the peak of the heat release rate occurs at 358ºCA (2ºCA before TDC). The premixed combustion occurs with a steep slope and it can be one of the major sources of NOx formation. The good agreement of predicted in-cylinder pressure with the experimental data [27] can be observed.

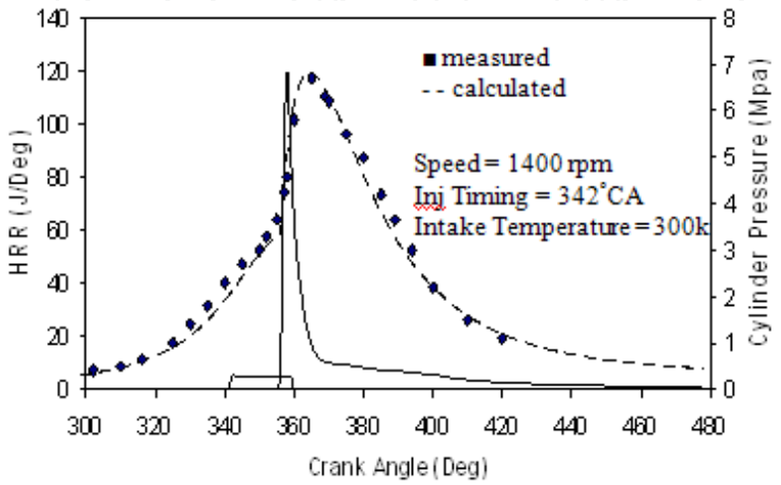

Figure 13. HRR and Comparison of calculated and measured [27] in-cylinder pressure, single njection case.

Fig. 14 and Fig. 15 imply that the predicted total in-cylinder NOx and soot emissions for the single injection case, agree well with the engine-out measurements [27].

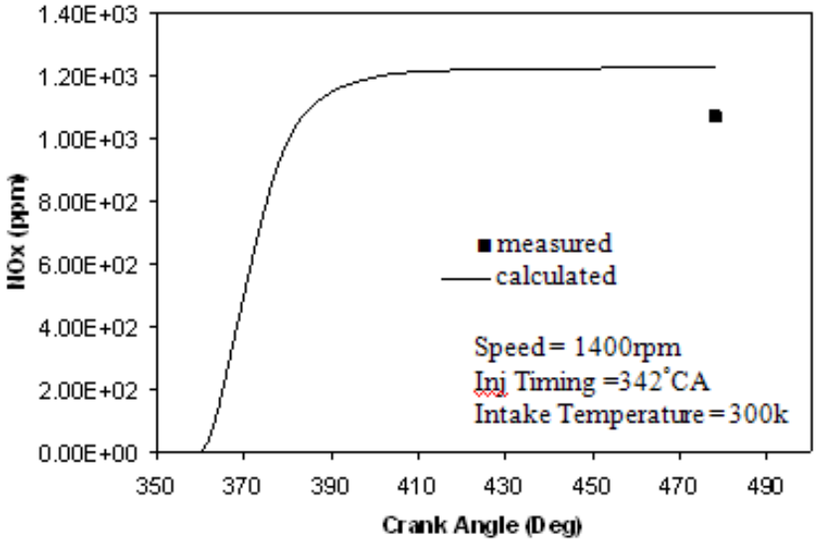

Figure 14. Comparison of calculated and measured [27] NOx emission, single injection case.

Fig. 16 shows the trade-off between NOx and soot emissions at EVO when the injection timing is varied. As indicated, the general trends of reduction in NOx and increase in soot when injection timing is retarded can be observed and it is independent on injection

strategy. The reason is that it causes the time residence and ignition delay to be shorter, resulting in a less intense premixed burn and soot formation increases; in addition, the less temperature in different parts of combustion chamber keeps the soot oxidation low but decreases the formation of thermal NOx.

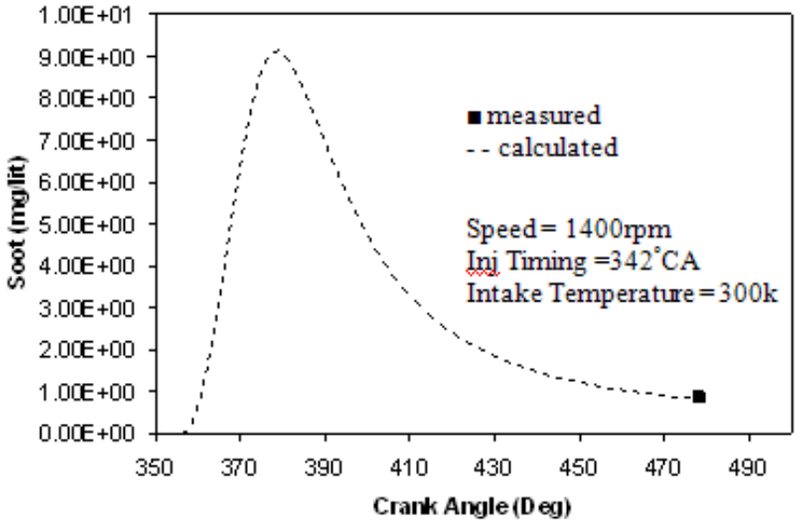

Figure 15. Comparison of calculated and measured [27] soot emission, single injection case.

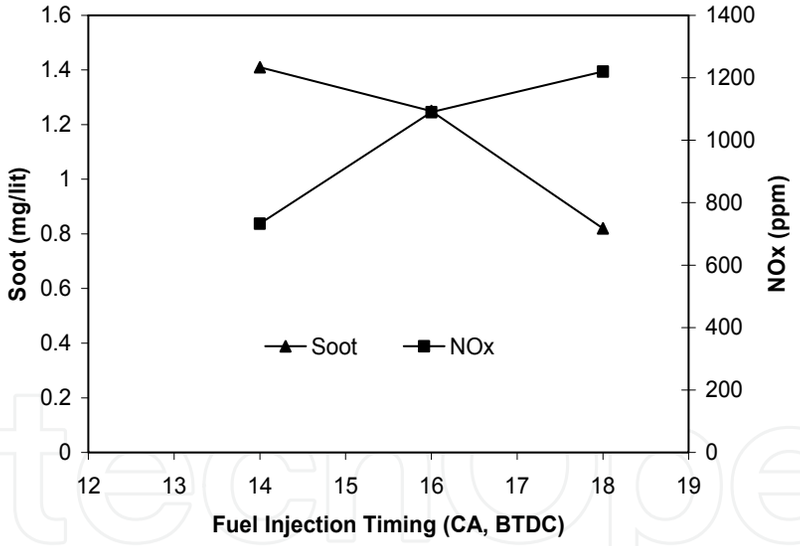

Figure 16. The effect of injection timing on NOx and Soot trade-off, single injection case.

To simulate the split injection, the original single injection profiles are split into two injection pulses without altering the injection profile and magnitude. In order to obtain the optimum dwell time between the injections, three different schemes including 10%, 20% and 25% of the total fuel injected in the second pulse are considered.

Fig. 17 shows the effect of delay dwell between injection pulses on soot and NOx emissions for the three split injection cases. For all the cases, the injection timing of the first injection pulse is fixed at 342ºCA.

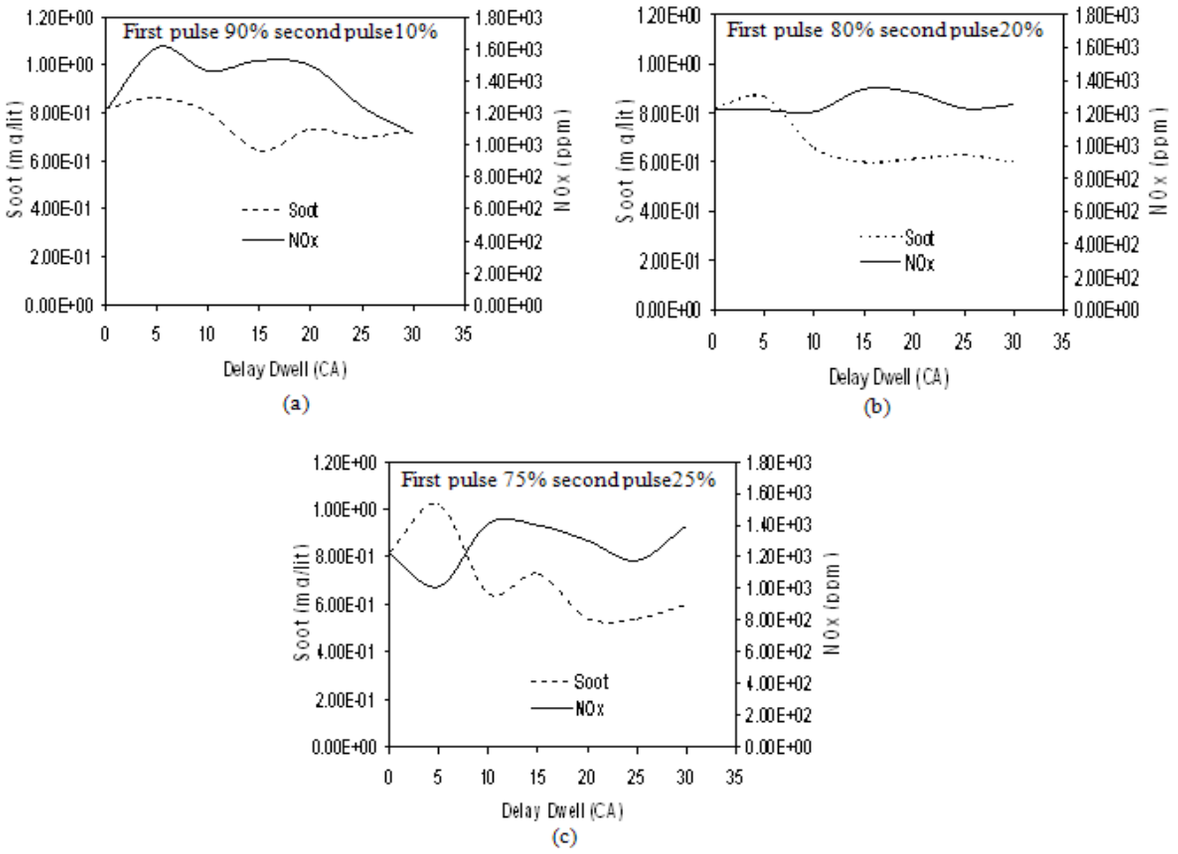

Figure 17. The variation of soot and NOx at different delay dwells, split injection cases.

The variation trend of curves in Fig. 17 is very similar to the numerical results obtained by Li et al [28]. As can be seen, the optimum delay dwell between the injection pulses for reducing soot with low NOx emissions is about 25ºCA. The evidences of Li, J. et al. [28], which has used a phenomenological combustion model, support this conclusion. Table 5 compares Exhaust NOx and soot emissions for the single injection and optimum split injection cases for the optimum delay dwell. As shown, for the 75% (25) 25% case, NOx and soot emissions are lower than the other cases. It is due to the fact that the premixed combustion which is the main source of the NOx formation is relatively low. The more quantity of the second injection pulse into the lean and hot combustion zones, causing the newly injected fuel to burn rapidly and efficiently at high temperatures resulting in high soot oxidation rates. In addition, the heat released by the second injection pulse is not sufficient to increase the NOx emissions. Fig. 18 and Fig. 19 confirm the explanations.

Case	NOx (ppm)	Soot (mg/lit)
Single inj	1220	0.82
Split inj- 90% (25) 10%	1250	0.697
Split inj- 80% (25) 20%	1230	0.614
Split inj- 75% (25) 25%	1180	0.541

Table 5. Comparison of NOx and soot emissions among the single injection and optimum split injection cases for the optimum delay dwell (25ºCA)

Fig. 18 shows the cylinder pressure and heat release rates for the three split injection cases in the optimum delay dwell i.e. 25ºCA. As shown, split injection reduces the amount of premixed burn compared to the single injection case in Fig. 13. The second peak which appears in heat release rate curves of split injection cases indicates that a rapid diffusion burn is realized at the late combustion stage and it affects the in-cylinder pressure and temperature. The calculated results of the cylinder pressure and HRR for the optimum split injection cases show very good similarity with the results of the reference[28].

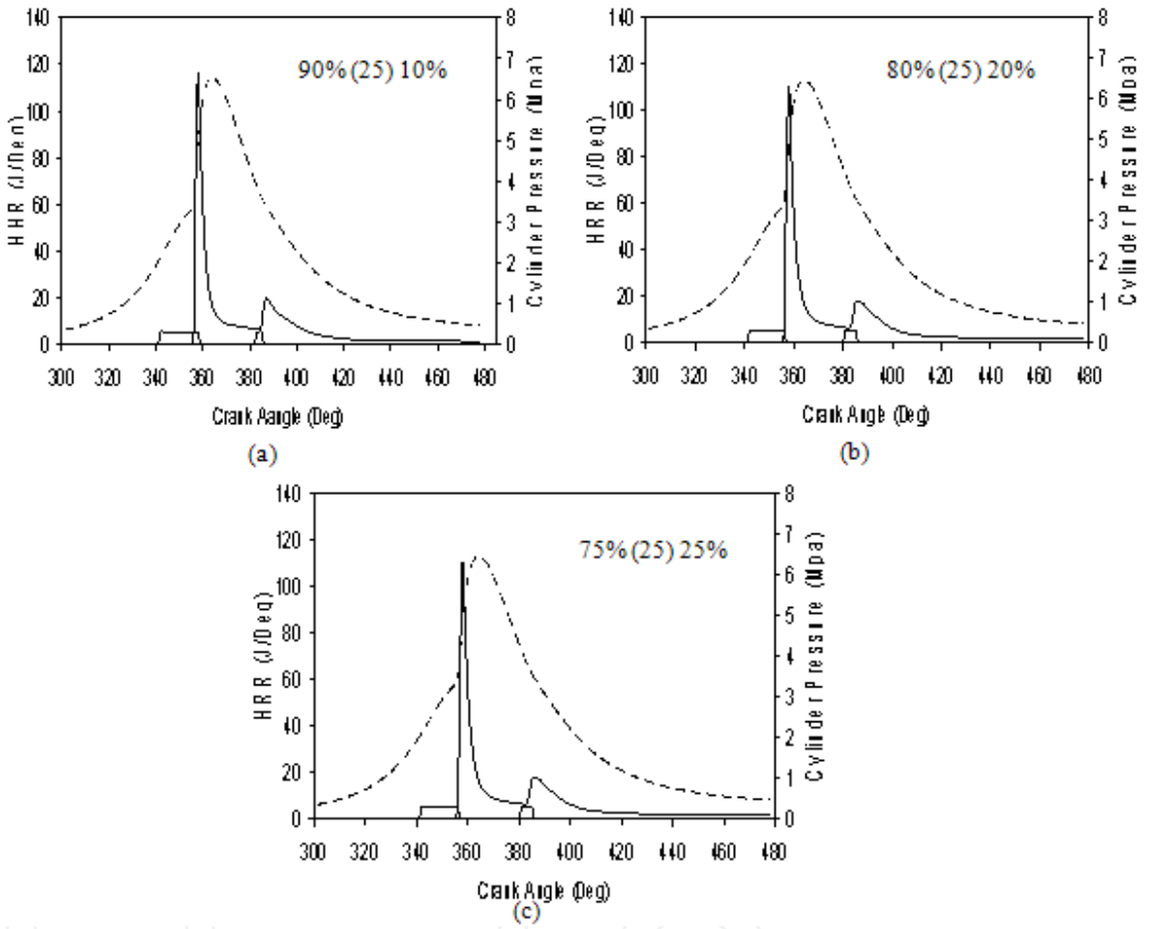

Figure 18. Cylinder HRR and pressure curves, optimum split injection cases.

Fig. 19 indicates the cylinder temperature for the single injection and optimum split injection cases. For the split injection cases, the two peaks due to the first and second injection pulses in contrast with the one peak in the single injection case can be observed. As shown, for the 75% (25) 25% case, the first and second peaks which are related to the premixed combustion and NOx formation are lower than the other cases. In addition, after the second peak, the cylinder temperature tends to increase more in comparison with the other cases and causes more soot oxidation. Hence, for the 75% (25) 25% case, NOx and soot emissions are lower than the other optimum cases.

Figure.20. shows the isothermal contour plots at different crank angle degrees for the 75% (25) 25% case at a cross-section just above the piston bowl. The rapid increase in

temperature due to the stoichiometric combustion can be observed at 355ºCA. At 360ºCA, the injection termination can be observed which the in-cylinder temperature tends to be maximum. At 370ºCA, the fuel injection has been cut off and the cylinder temperature tends to become lower. As described, injection termination and resumption prevents not only fuel rich combustion zones but also causes more complete combustion due to better air utilization. The resumption of the injection can be observed at 380ºCA which causes the diffusion combustion and increases the temperature in the cylinder. At 390ºCA, the increase of cylinder temperature creates bony shape contours and soot oxidation increases.

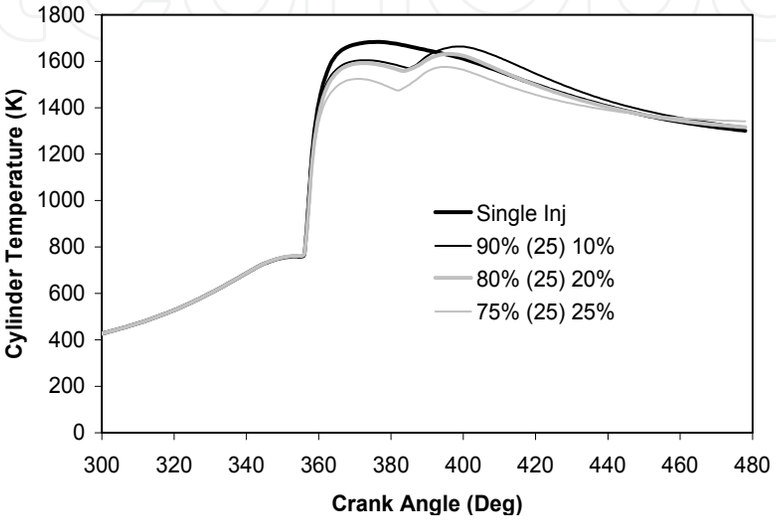

Figure 19. Comparison of cylinder temperature among the single injection and optimum split injection cases.

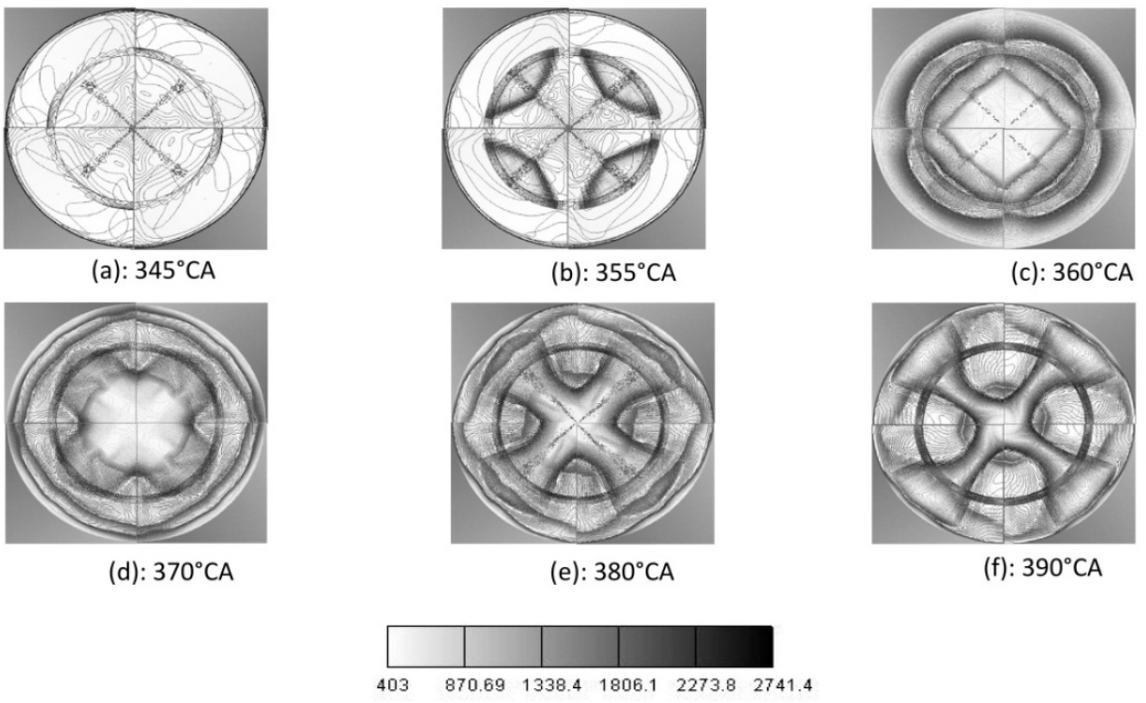

Figure 20. Isothermal contour plots of 75% (25) 25% case at different crank angle degrees.

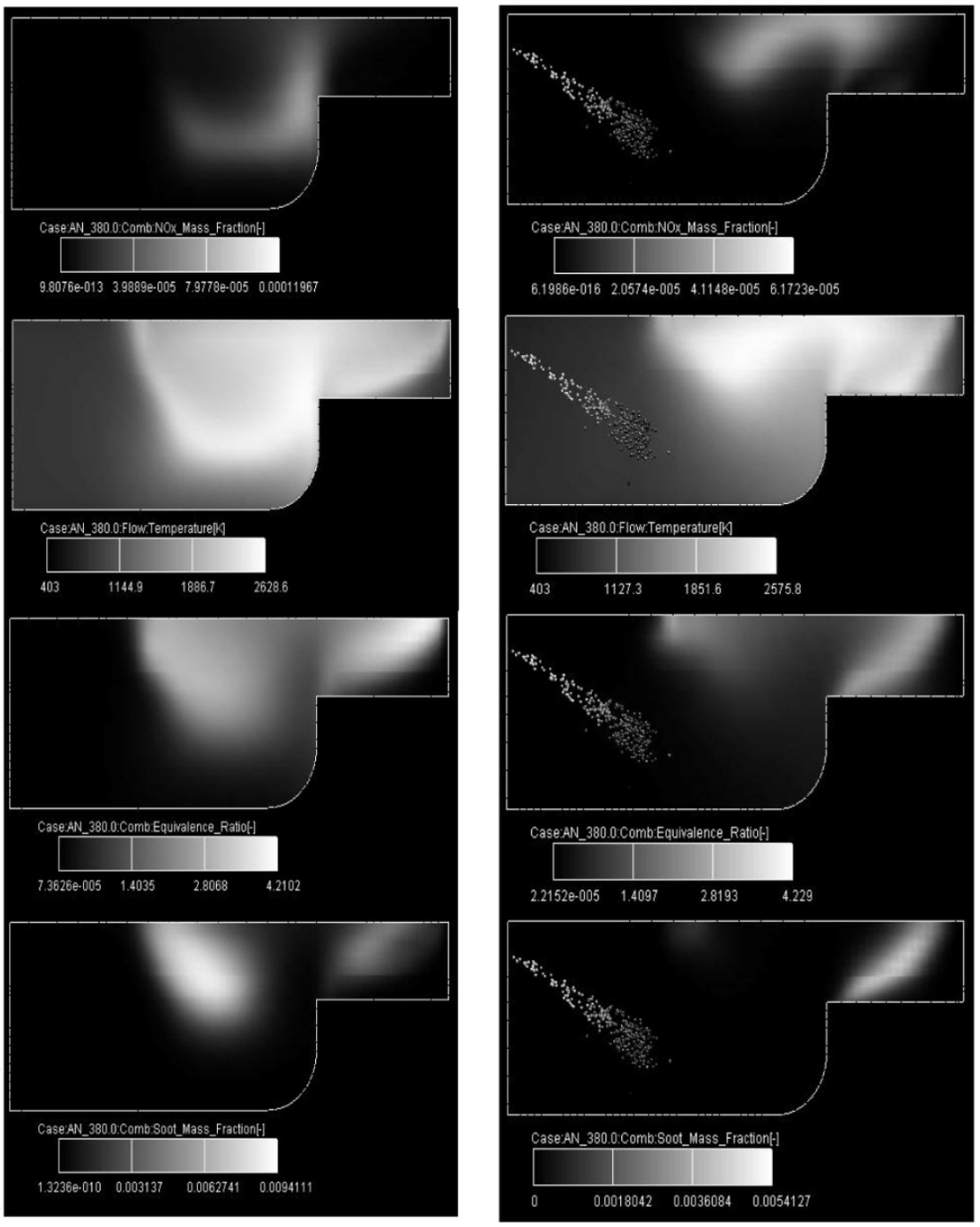

Figure 21. Contour plots of NOx, temperature, equivalence ratio, and soot with fuel droplets at 380°CA for the single injection and 75% (25) 25% cases.

Fig. 21 compares the contour plots of NOx, temperature, equivalence ratio and soot for the single injection and 75% (25) 25% cases in a plane through the center of the spray at 380ºCA. As explained above, 380ºCA corresponds to a time when the second injection pulse has just started for the 75% (25) 25% case. For the two described cases, it can be seen that the area which the equivalence ratio is close to 1 and the temperature is higher than 2000 K is the

NOx formation area. In addition, the area which the equivalence ratio is higher than 3 and the temperature is approximately between 1600 K and 2000 K is the soot formation area. A local soot-NOx trade-off is evident in these contour plots, as the NOx formation and soot formation occur on opposite sides of the high temperature region. It can be seen that for the 75% (25) 25% case, NOx and soot mass fractions are lower in comparison with the single injection case. Because of the optimum delay dwell, the second injection pulse, maintains the low NOx and soot emissions until EVO.

7. Conclusion

At the present work, the effect of the split injection on combustion and pollution of DI and IDI diesel engines was studied at full load state by the CFD code. The target was to obtain the optimum split injection cases for these engine in which the total exhaust NOx and soot concentrations are the lowest.

Three different split injection schemes, in which 10, 20 and 25% of total fuel injected in the second pulse, was considered. The delay dwell between injections pulses is varied from 5°CA to 30°CA with the interval 5°CA.The results for IDI are as followed:

1. The calculated combustion and performance parameters, exhaust NOx and soot emissions for the single injection case showed a good agreement with the corresponding experimental data.
2. The lowest NOx and Soot emissions are related to the 75%-15-25% and 75%-20-25% cases respectively. Finally, optimum case was 75%-20-25% regarding the highest average of NOx and soot reduction.
3. The lowest brake power and highest BSFC quantity is due to the 75%-30-25% case.
4. Because in the literature, the optimum split injection scheme for DI diesel engines at full state was defined as 75%-25-25%, it was concluded that the difference of the optimum split injection scheme for DI and IDI diesel engines was related to the delay dwell between the injections.
5. The main difference of the in-cylinder flow field between the single injection and split injection cases is due to the fuel injection scheme.
6. For the 75%-20-25% case, the more availability of oxygen in the expansion stroke compensates the decrease of temperature due to the split injection. Hence, soot oxidation is increased.
7. The final form of the NOx and soot at 420°CA which preserve it's trend until EVO, confirms the more reduction of NOx and soot for the 75%-20-25% case in comparison with the single injection case.

In addition, the results for DI engins are as follow:

1. A good agreement of predicted in-cylinder pressure and exhaust NOx and soot emissions with the experimental data can be observed.
2. Advancing or retarding the injection timing can not decrease the soot and NOx trade-off by itself. Hence split injection is needed.

3. The optimum delay dwell between the injection pulses for reducing soot with low NOx emissions is about 25ºCA. The results of phenomenological combustion models in the literature support this conclusion.
4. The calculated results of the cylinder pressure and heat release rate for the optimum split injection cases show very good similarity with the numerical results obtained by phenomenological combustion models.
5. For the 75% (25) 25% case, NOx and soot emissions are lower than the other cases. It is due to the fact that the premixed combustion which is the main source of the NOx formation is relatively low. The more quantity of the second injection into the lean and hot combustion zones, causing high soot oxidation rates. In addition, the heat released by the second injection pulse is not sufficient to increase the NOx emissions.
6. Contour plots of NOx, temperature, equivalence ratio and soot for the single injection and 75% (25) 25% cases at 380ºCA show that the area which the equivalence ratio is close to 1 and the temperature is higher than 2000 K is the NOx formation area. In addition, the area which the equivalence ratio is higher than 3 and the temperature is approximately between 1600 K and 2000 K is the Soot formation area.

Abbreviations

BTDC	before top dead center
ATDC	after top dead center
EVO	exhaust valve opening
IDI	indirect injection engine
CA	crank angle
SOC	start of combustion
HRR	heat release rate
ID	ignition delay
BSFC	brake specific fuel consumption
ABDC	after bottom dead center
BBDC	before bottom dead center
BMEP	brake mean effective pressure

Author details

S. Jafarmadar
Mechanical Engineering Department, Technical Education Faculty, Urmia University, Urmia, West Azerbaijan, Iran

8. References

[1] Gomaa M, Alimin AJ, Kamarudin KA. Trade-off between NOx, soot and EGR rates for an IDI diesel engine fuelled with JB5. World Academy of Science, Engineering and Technology 2010; 62:449-450.

[2] Bianchi GM, Peloni P, Corcione FE, Lupino F. Numerical analysis of passenger car HSDI diesel engines with the 2nd generation of common rail injection systems: The effect of multiple injections on emissions. SAE Paper NO. 2001-01-1068; 2001.
[3] Seshasai Srinivasan, Franz X. Tanner, Jan Macek and Milos Polacek. Computational Optimization of Split Injections and EGR in a Diesel Engine Using an Adaptive Gradient-Based Algorithm. SAE paper, 2006-01-0059
[4] Shayler Pj, Ng HK. Simulation studies of the effect of fuel injection pattern on NOx and soot formation in diesel engines. SAE Paper NO. 2004-01-0116; 2004.
[5] Chryssakis CA, Assanis DN, Kook S, Bae C. Effect of multiple injections on fuel-air mixing and soot formation in diesel combustion using direct flame visualization and CFD techniques. Spring Technical Conference, ASME NO. ICES2005-1016; 2005.
[6] Lechner GA, Jacobs TJ, Chryssakis CA, Assanis DN, Siewert RM. Evaluation of a narrow spray cone angle, advanced injection strategy to achieve partially premixed compression ignition combustion in a diesel engine. SAE Paper No. 2005-01-0167; 2005.
[7] Ehleskog R. Experimental and numerical investigation of split injections at low load in an HDDI diesel engine equipped with a piezo injector. SAE Paper NO. 2006-01-3433; 2006.
[8] Sun YD, Reitz R. Modeling diesel engine NOx and soot reduction with optimized two-stage combustion. SAE Paper No. 2006-01-0027; 2006.
[9] Verbiezen K. et al. Diesel combustion: in-cylinder NO concentrations in relation to injection timing. Combustion and Flame, 2007; 151:333–346.
[10] Abdullah N, Tsolakis A, Rounce P, Wyszinsky M, Xu H, Mamat R. Effect of injection pressure with split injection in a V6 diesel engine. SAE Paper NO. 2009-24-0049; 2009.
[11] Jafarmadar S, Zehni A. Multi-dimensional modeling of the effects of split injection scheme on combustion and emissions of direct-injection diesel engines at full load state. IJE, 2009; Vol. 22, No. 4.
[12] Showry K, Raju A. Multi-dimensional modeling and simulation of diesel engine combustion using multi-pulse injections by CFD. International Journal of Dynamics of Fluids 2010; ISSN 0973-1784 Vol 6, NO 2, p. 237–248.
[13] Iwazaki K, Amagai K, Arai M. Improvement of fuel economy of an indirect (IDI) diesel engine with two-stage injection. Energy Conversion and Management, 2005; 30:447-459.
[14] AVL FIRE user manual V. 8.5, 2006.
[15] Han Z, Reitz R D.Turbulence modeling of internal combustion engines using RNG K-ε models. Combustion Science and Technology 1995; 106, p. 267-295.
[16] Liu AB, Reitz RD. Modeling the effects of drop drag and break-up on fuel sprays. SAE Paper NO. 930072; 1993.
[17] Dukowicz JK. Quasi-steady droplet change in the presence of convection. Informal report Los Alamos Scientific Laboratory. LA7997-MS.
[18] Naber JD, Reitz RD. Modeling engine spray/wall impingement. SAE Paper NO. 880107; 1988.

[19] Halstead M, Kirsch L, Quinn C. The Auto ignition of hydrocarbon fueled at high temperatures and pressures - fitting of a mathematical model. Combustion Flame 1977; 30:45-60.

[20] Patterson MA, Kong SC, Hampson GJ, Reitz RD. Modeling the effects of fuel injection characteristics on diesel engine soot and NOx emissions. SAE Paper NO. 940523; 1994.

[21] Khoushbakhti Saray R, Mohammahi Kusha A, Pirozpanah V. A new strategy for reduction of emissions and enhancement of performance characteristics of dual fuel engine at part loads. Int. J. Engineering 2010; 23:87-104.

[22] Heywood JB. Internal combustion engine fundamental. New York: McGraw Hill Book Company; 1988, p. 568-586.

[23] Sbastian S, Wolfgang S. Combustion in a swirl chamber diesel engine simulation by computation of fluid dynamics. SAE Paper NO. 950280; 1995.

[24] Yoshihiro H, Kiyomi N, Minaji I. Combustion improvement for reducing exhaust emissions in IDI diesel engine. SAE Paper NO. 980503; 1998.

[25] Hajireza S, Regner G, Christie A, Egert M, Mittermaier, H. Application of CFD modeling in combustion bowl assessment of diesel engines using DoE methodology. SAE Paper NO. 2006-01-3330; 2006.

[26] Carsten B. Mixture formation in internal combustion engines. Berlin: Springer publications; 2006, p. 226-231.

[27] Pirouzpanah, V. and Kashani, B. O., "Prediction of major pollutants emission in direct-injection dual-fuel diesel and natural gas engines", SAE Paper, NO. 1999-01-0841, (1999).

[28] Li, J., Chae, J., Lee, S. and Jeong, J. S., "Modeling the effects of split injection scheme on soot and NOx emissions of direct injection diesel engines by a phenomenological combustion model", SAE Paper, NO. 962062, (1996).